Bio-based ablative thermal protection materials for space application

Raphaela Günther[a], Oliver Hohn[b], Holger Unbehaun[c], Oliver Drescher[d], Hendrik Weihs[e]

[a]*Dresden University of Technology (TUD), Chair of Space Systems, 01307 Dresden, Germany*
[b]*German Aerospace Center (DLR), Supersonic and Hypersonic Technologies Department, 51147 Köln, Germany*
[c] *Dresden University of Technology (TUD), Chair of Wood and Fibre Material Technology, 01307 Dresden, Germany*
[d]*German Aerospace Center (DLR), Mobile Rocket Base (MORABA), 82234 Weßling, Germany*
[e]*German Aerospace Center (DLR), Institute for Structures and Design, 70569 Stuttgart, Germany*

Abstract

In the context of a growing bioeconomy, green renewable resources are of interest for the space industry. Because of its relatively low density, low thermal conductivity, easy handling and good ablative behaviour bio- and wood-based materials are taken into consideration for the use as a thermal protection system (TPS) material on hot structures such as the leading edges of stabilising fins, fairings, nose cones and other TPS applications. As a mandatory and thus flight critical structure of launch vehicles, these parts need to be aerodynamically effective, lightweight, stiff and heat resistant on its foremost front end, where high temperatures may arise from gas kinetic effects.

In order to gain a deeper understanding and assess the applicability of modern bio- and wood-based materials, a systematic literature and patent analysis of bio- and wood-based materials in spaceflight has been conducted as a starting point for the research. To set a framework for the application of a bio-based material in space, functionality and boundary conditions have been analysed and form requirements for the development of the bio-based TPS material. Further, prototype materials with varying ingredients of natural fibres, binders and additives have been developed and characterised by a thermogravimetric analysis (TGA) to determine their general suitability as a TPS material. The materials have been additionally screened in more detail via the analyses of bulk density, thermal conductivity and specific heat capacity. Measurements under real environmental conditions in a plasma channel were carried out for further investigation and form the core of this

work. With the defined requirements and results from screening tests and plasma channel tests a selection of the best-performing prototype material could be made. First impacts on launch vehicle's design and an outlook for future research on bio-based TPS conclude this contribution.

Keywords: bio-based, renewable resources, ablation, thermal protection, TPS, re-entry

1 Introduction and motivation

The current shift in the space industry towards the development of smaller payloads brings greater flexibility and opens up numerous approaches and opportunities for the development of innovative launch vehicles [1]. In the context of a growing bioeconomy, green renewable resources are of interest for the space industry. They have the potential of being future substitute materials for a CO_2-neutral economy, decreasing debris in space and on Earth, and paving the way to a circular space economy.

Due to the increasing need to launch smaller payloads and sounding rocket experiments more frequently, a greater demand of small launch vehicles and sounding rockets arises [2]. At the same time, the construction of new launch vehicles is accompanied by an increased consumption of material resources. Mainly, most of the launch vehicle's hardware is designed to be non-reusable after the mission, due to a low cost and high efficiency approach of the launch vehicle operator. Only the most valuable scientific payload and payload support systems are commonly recovered and refurbished for re-flights, which are marked in red as an example for the VSB-30 two-stage sounding rocket vehicle in Figure 1. Considering these circumstances, the sustainability of the launch vehicle, especially the use of raw renewable materials and green manufacturing processes, becomes a compelling issue for components that are disposed after each vehicle operation and not recovered. Therefore, it is particularly interesting for single-use components to investigate how the potential of natural, renewable materials can be used and optimized in space engineering and on launch vehicles with regard to sustainability aspects.

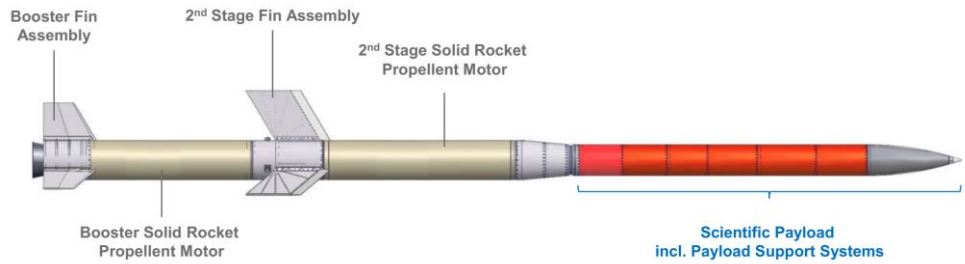

Figure 1: DLR Mobile Rocket Base (MORABA) VSB-30 two-stage sounding rocket vehicle

Various hot structures can be assigned to single-use components, such as the leading edges of stabilising fins, fairings or nose cones. These components are essential structural components for a stable, aerodynamic flight. Therefore, they have to withstand high thermal and mechanical loads, be characterized by high stiffness and at the same time, should have a relatively low mass. Especially on their foremost front end, where high temperatures may arise from gas kinetic effects, these components must be heat resistant and form stable.

A common solution for overheating components, especially for fin leading edges, can be the use of high temperature steel alloys, thermal protection system (TPS) layers or their combination. The steel version needs to be lightweight, thus almost only sheet metal comes into consideration, revealing to be critical in terms of thermal stress relief deformations effecting the vehicle's flight mechanical performance. Layers of TPS around the leading edge need to be relatively thin and hence are rapidly degrading leaving the underlying structure unprotected during later flight phases. Figure 2 demonstrates both effects for a typical VSB-30 flight where a combination of steel sheet metal leading edges with an ablative TPS was used.

Consequently, the German Aerospace Center (DLR) Institute of Structures and Design developed special phenolic glass fibre reinforced leading edges, which were introduced by DLR MORABA on all their thermally higher loaded fin assemblies. Even though this material serves the temperature load as well as the component's major specifications in a more appropriate way, its lack of lightweight design and sustainability as a renewable, "green" material are immanent.

Figure 2: Thermal load on fin leading edges after 2nd stage burn of DLR MORABA sounding rocket vehicle (left) and 2nd stage fin with steel sheet metal leading edge and ablative TPS recovered after VSB-30 flight operation

Here lies the potential of bio- and wood-based materials. They are considered for the application as a TPS material on hot structures due to their relatively low density, low thermal conductivity, lightweight construction properties, easy handling, good biodegradability and good ablative behaviour. However, sounding rockets are a very suitable test bed to verify component's material and structural concepts for all other launch systems. Therefore, for studying a potential application of bio-based ablative thermal protection materials in space, the fin leading edge of a sounding rocket was chosen as a component for first investigations.

The research was conducted by Dresden University of Technology (TUD) in collaboration with the German Aerospace Center (DLR). For the investigation, the DLR STORT flight envelope was taken as a reference, since it is one of the most thermally and mechanically demanding high-altitude research flights for DLR MORABA [3]. Thus, the limits of the material candidates can be extensively explored. The investigation will consider solid wood and wood fibre materials to identify preferred material variants for an application on fin leading edges of sounding rockets. For comparison a phenolic glass fibre reinforced material (comparative material 1, CM 1) and a high temperature steel alloy (comparative material 2, CM 2), which are already applied on sounding rockets, are used.

2 Requirement analysis

For the requirement analysis three aspects are taken into consideration. The requirements of fin leading edges in general, optional requirements of fin leading edges from natural origin and additional requirements for natural fibre-based fin leading edges.

General requirements for fin leading edges formulated by DLR MORABA are:

- The fin leading edges shall be fail-safe at all times during the mission.
- The fin leading edges shall support aerodynamic loads of the STORT mission in medium range and thermal loads in high range.
- The fin leading edges geometry and integrity shall maintain over a long period of the flight.

Optional requirements for fin leading edges from natural origin formulated by DLR MORABA are:

- The bio-based fin leading edge shall have a lower mass.
- The bio-based fin leading edge shall have an improvement in flight stability.
- The bio-based fin leading edge shall reduce the flutter behaviour.
- The bio-based fin leading edge shall reduce the polar moment of inertia.
- The bio-based fin leading edge shall have lower production cost.
- The bio-based fin leading edge shall reduce the requirements for post-flight NDI or structural health monitoring.

Additional requirements for bio-based fin leading edges identified by TUD are:

- Bio-based fin leading edges shall have high material strengths and densities to maintain structural integrity under mechanical and high thermal loads.
- Bio-based fin leading edges shall have low thermal conductivity and high thermal resistance to prevent heat transfer throughout the fin structure
- Bio-based fin leading edges shall maintain their geometry.

3 Material screening and selection

The materials to be tested should represent a wide range of material properties within their material type. Thus, the materials can be compared with each other in a more differentiated manner. As natural fibre-based materials, the materials solid wood, wood fibre materials and cork are selected. As solid woods, both softwoods and hardwoods are selected. In the case of wood fibre materials, industrial material (I-WBM) is compared with material produced by TUD (TUD-WBM-0, TUD-WBM-1 and TUD-WBM-2). Among the possible tropical and native woods, domestic wood species are preferred for an application in an European sounding rocket, as they are readily available in Europe and reduce CO_2 emissions during harvesting, transport and logistics. Therefore, only regional, native wood species are considered in the material selection.
To identify most suited wood fibre materials for an application on fin leading edges, screening tests were carried out for the test material selection. As the main stress on the leading edge of the fin is caused by thermal loads and the temperature resistance of the fin edge is a general requirement, analyses to characterize thermal material properties form the basis for the selection of the material.

3.1 Preliminary test

The evaluation of a preliminary test serves as experimental basis. Two test specimens made of solid woods (oak (PT-oak) and mahogany (PT-mahogany)), specimens of a preliminary test material 1 (PTM-1) based on carbon fibres and a preliminary test material 2 (PTM-2) based on a phenolic glass fibre reinforced composite were tested in the arc-heated wind tunnel L2K of the Institute of Aerodynamics and Flow Technology, Supersonic and Hypersonic Technologies (DLR). In addition to a mass and a cross-sectional area analysis, a microscopic analysis of micrographs was conducted.
A clear correlation between the anatomy of the wood species and their behaviour under thermal load can be seen. The large differences in pore size between early and late wood as well as thicker wood strands cause a stronger degradation of the material. The orientation of the wood structure, especially the wood rays to the direction of load determines the burning behaviour. A uniform pore size, distribution of pores within the material, and a small difference between early and late wood, seem to prevent severe burning and support a more stable porous char layer.

3.2 Thermogravimetric analysis (TGA)

Particular focus was placed on a TGA as a fundamental screening tool, which provides information on the char yield and pyrolytic behaviour of a material by determining the change in mass of a test material as a function of temperature and time. The TGA was performed with the test materials listed in Table 1.

Table 1: Test materials for TGA

Test material	Material specifications	Further information
I-WBM	industrial wood-based material	contains flame retardant
TUD-WBM-0	wood-based material produced at TUD	100 % wood fibre, flame retardant free
TUD-WBM-1	wood-based material produced at TUD	100 % wood fibre, contains bio-based flame retardant
TUD-WBM-2	wood-based material produced at TUD	wood fibre and special natural fibre material, contains bio-based flame retardant
Oak	solid wood hard wood	*Quercus petraea, Q. robur*
Larch	solid wood, soft wood	*Larix decidua, Larix* spp.

The measurements were carried out in two steps:

1. The pre-dried test specimens were heated in the TGA test device with a temperature increase of 15 K/min from 25 °C to 105 °C.
2. The test specimens were heated from 105 °C to 1000 °C at 40 K/min.

During the measurement, a nitrogen atmosphere with a volume flow of 3.5 l/min prevailed in the measuring device.

The visual test results are displayed each before and after the analysis in Figure 3. The black and cracked or porous surfaces of the TUD-WBM-1 (top row left) and I-WBM samples (top row right) can be seen. The surfaces of the TUD-WBM-2 (middle row left) show light-coloured, mineral deposits. The test specimen of TUD-WBM-0 (middle row right) show a significant loss in volume and a dark, charred surface. All wood fibre materials retain their materials' cohesion. The test specimen of the solid wood oak (bottom row left) and larch (bottom row right) are structurally very degraded or disjointed. A partially charred and ashen, fragile surface can be seen.

Figure 3: Test specimens each before (right) and after (left) TGA

A clear mass loss for all test specimens at 1000 °C can be seen in Figure 4. The pre-drying results in a negligible mass loss due to the evaporation of water, as the data curves are nearly constant until 120 °C. Therefore, it can be deducted that the mass losses shown are exclusively caused by the ingredients of the test materials. The test specimens made of solid wood retain their mass up to a temperature of about 200 °C, after which it drops very steeply to less than 20 % (larch) and less than 30 % (oak). The TUD-WBM-0 test specimens have slightly higher residual mass percentages above 30 % compared to the solid wood test specimens. The I-WBM and TUD-WBM-1 test specimens still have 30 - 35 % of their original mass when they reach 1000 °C. Within the same material, the curves of mass loss are approximately similar. Comparing the curves of TUD-WBM-0 and TUD-WBM-1, it becomes evident that the use of flame retardant has a positive effect on mass loss. With above 40 %, the TUD-WBM-2 test specimens show the highest residual mass ratio. This result can be explained by the materials composition. The natural salts, sandy residues and suspended matter contained in the special natural fibre material have high melting points (sodium chloride/ salt: $T_M \sim 801$ °C [4], quartz sand: $T_M \sim 1713$ °C [5]), slowing down the materials' decomposition and thus acting as natural flame retardants. These not decomposed components form the light-coloured, mineral deposits as seen in Figure 3 on the test specimen surface.

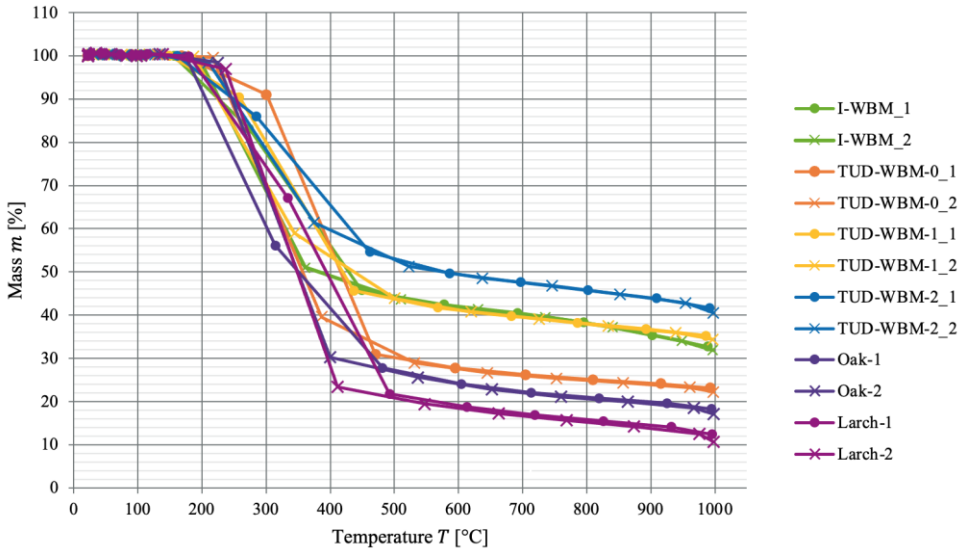

Figure 4: Test results of TGA

3.3 Thermal material characterization

For the newly at TUD developed wood-based materials the bulk density, thermal conductivity and specific heat capacity were determined for the material screening. The results and literature values for the remaining materials are shown in Table 2.

Table 2: Properties of test materials

Material	Bulk density ρ (g/cm^3)	Thermal conductivity λ (W/mK)	Specific heat capacity c_p (J/kgK)
I-WBM	0.80	0.225	1446.0
TUD-WBM-1	0.87 [+]	0.353 (plane)	1467.7
TUD-WBM-2	0.89 [+]	0.252	1493.2
Oak	0.71 [6] 0.66[+]	0.166 [7]	-
Larch	0.60 [6] 0.55 [+]	0.114 [7]	-
CM 1	2.0 ± 0.1	0.4 ± 0.1	> 850
CM 2	7.9	15	500

[+] Measurements at TUD

The thermal conductivities of all wood fibre materials are less than half the thermal conductivities of CM 1 and CM 2. This means that the natural fibre-based materials insulate heat better and transfer less heat to the fin when used in fin leading edges. Compared with literature values of $\lambda = 0.18$ W/mK according to DIN EN ISO 10456 for wood fibre boards with bulk densities of 0.8 g/cm^3 [8], the analysed materials have higher thermal conductivities.
The values of the specific heat capacity of all analysed materials are very similar. The specific heat capacities of the wood fibre materials are more than twice (CM 1) or three times (CM 2) as large as those of previously used materials. This means that the natural fibre-based materials can store heat better or have a lower temperature rise in the material. For the use of these materials in fin leading edges, more heat would be required to heat the material compared to the fin leading edge materials used so far. Compared to literature values of c_p = 1700 W/mK according to DIN EN ISO 10456 for wood fibre boards with bulk densities of 0.8 g/cm^3 [8], the analysed materials have lower specific heat capacities.

3.4 Material selection

Based on the screening tests and especially under consideration of the TGA results, materials for testing in the plasma channel L2K were selected. The test specimens for L2K of the selected materials are shown in Figure 5.

As solid woods, two hardwoods (oak and birch) and one softwood (larch) were chosen. Because hardwoods have higher average strengths and bulk densities, more hardwoods than softwoods were chosen. Oak was selected as a ring-porous wood with a high bulk density of 0.71 g/cm^3 [6] and birch as a dispersed-porous wood due to its high elasto-mechanical properties. Larch, with a bulk density of 0.6 g/cm^3 [6], has the highest bulk density of all European softwood species, making it the heaviest and hardest native softwood. Due to a deviating origin and regionality of the solid woods, the calculated density of, for example, oak for test specimens of the preliminary test (ρ = 0.83 g/cm^3) is higher than that of oak for the test specimens (ρ = 0.66 g/cm^3).

For the wood-based materials, an industrially produced fibreboard material I-WBM was selected, which was developed for increased fire protection requirements in non-load-bearing interior applications in dry areas. In the context of the investigations, it represents an industrial comparative material. The TUD-WBM-1 and TUD-WBM-2 materials from TUD were also selected. For wood fibre materials, they have high average bulk densities of 0.87 g/cm^3 and 0.89 g/cm^3.

Figure 5: Test specimen of selected material

4 Plasma testing

In the scope of testing, the test facility, the test conditions and test specimens are described below. Further, test results are presented.

4.1 Test facility – arc-heated wind tunnel L2K

The arc-heat wind tunnel facilities LBK of DLR are certified by ESA as a European key facility for testing and qualification of thermal protection systems. The LBK facilities consist of two nearly independent test legs, called L2K and L3K. The setup of the facilities is schematically plotted in Figure 6. The two legs share a common system of vacuum pumps and exhaust gas cleaning as well as the low-pressure cooling cycle for the test chamber and the heat exchangers in the diffusors. Apart from this, the facilities can operate independently as each is equipped with their own power and gas supply, arc

heater cooling systems and controls. The L2K facility is equipped with a Huels-type arc heater for gas mass flow rates between 5 and 75 g/s. With a maximum power of 1.4 MW moderate specific enthalpies up to 10 MJ/kg are achieved at a gas mass flow rate of 50 g/s, which corresponds to a reservoir pressure of about 1500 hPa. As the working gases, air, nitrogen, argon or mixtures thereof e.g. for Martian (CO_2/N_2) or Titan (N_2/CH_4) atmospheres can be used.

Hypersonic free stream velocities are provided by a convergent-divergent nozzle. The nozzle's expansion part is conical with a half angle of 12°. Different throat diameters from 14 mm to 29 mm are available and can be combined with nozzle exit diameters of 50 mm, 100 mm, and 200 mm. Consequently, the facility setup can effectively be adapted to particular necessities of a certain test campaign [9–11].

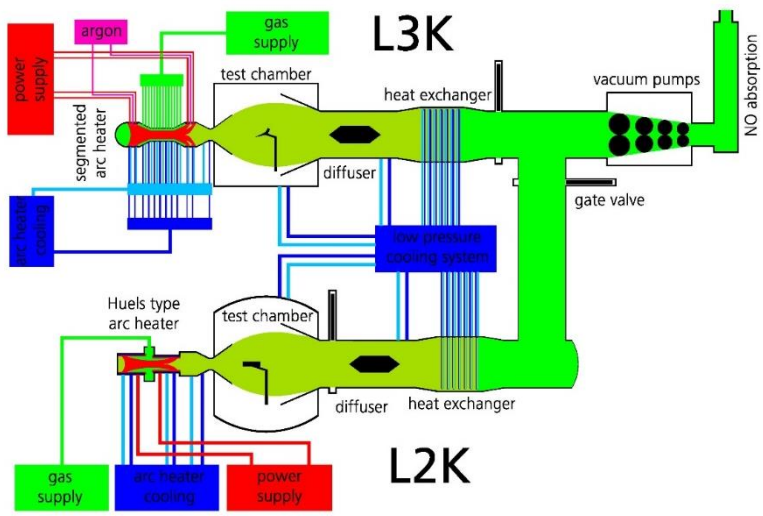

Figure 6: Schematic overview of the arc-heated wind tunnel facilities LBK

4.2 Test condition and test specimens

The test condition was chosen to represent the case of maximum total enthalpy encountered during the projected STORT flight trajectory which occurs at an altitude of approximately 41.5 km at a flight Mach number of 8.6 [3]. At this point the vehicle experiences a total enthalpy of about h_0 = 4.048 MJ/kg at a stagnation pressure of p_s = 254 hPa.

With these values, the parameter

$$h_0 \cdot \sqrt{p_s} \sim 64.5 \qquad (1)$$

can be calculated as a reference value for the thermal load, when h_0 is entered in the unit MJ/kg and p_s in hPa. This parameter can then be used as a similarity parameter for determining the wind tunnel conditions. Furthermore, it has to be considered that the flow in L2K is in thermal and chemical non-equilibrium with a rather high portion of atomic oxygen from dissociation in the arc-heater, when air is used as a test gas, whereas in real flight, the portion of atomic oxygen is very small (<< 1 %). In order to account for these factors, the condition in Table 3 with a mixture of 96 % nitrogen and 4 % air was used for the wind tunnel tests.

Table 3: Test conditions for L2K experiments

Flow parameter	Value
Total gas mass flow [g/s]	50
Air mass flow [g/s]	2
Nitrogen mass flow [g/s]	48
Total enthalpy [MJ/kg]	6.85
Stagnation pressure [hPa]	89
$h_0 \cdot \sqrt{p_s}$	64.6
Nozzle configuration (throat/exit diameter) [mm]	29/100
Distance from nozzle exit [mm]	120
Test duration [s]	120

The test specimens made of the selected materials consist entirely of solid material. The materials that showed the least degradation were tested three times. Thus, reliability was increased in the testing. The multiple tested materials include I-WBM, TUD-WBM-1 and TUD-WBM-2. The test specimens do not have temperature sensors integrated into the sample structure. The sample geometry used results from the defined fin leading edge geometry. During the tests, the test specimens are clamped into a cooled sample holder, which is fixed in the test chamber of the L2K. A water-based cooling system ensures uniform removal of heat from the sample holder during measurements and guarantees firm clamping at the applied thermal loads.

4.3 Test results

The boundary layer that forms around the test specimen during testing is seen in Figure 7. In the upper half of the image, the mechanical surface erosion of the ablation shows the removal of a material particle that is carried away from the test specimen by the free plasma flow. The test specimen tips of TUD-WBM-2 and oak are shown on the right side Figure 7. At the TUD-WBM-2 test specimen the annealing of the test specimen tip and the formation of melt beads from the resins and mineral components contained can be seen. The pointed shape and straight fin leading edge were maintained throughout the test period. The tip of the oak test specimen decomposes irregularly compared to TUD-WBM-2 and does not form a straight leading edge. The pointed test specimen shape cannot be maintained over the test duration of 120 s. A detachment of porous carbon can be seen on the upper part of the test specimen.

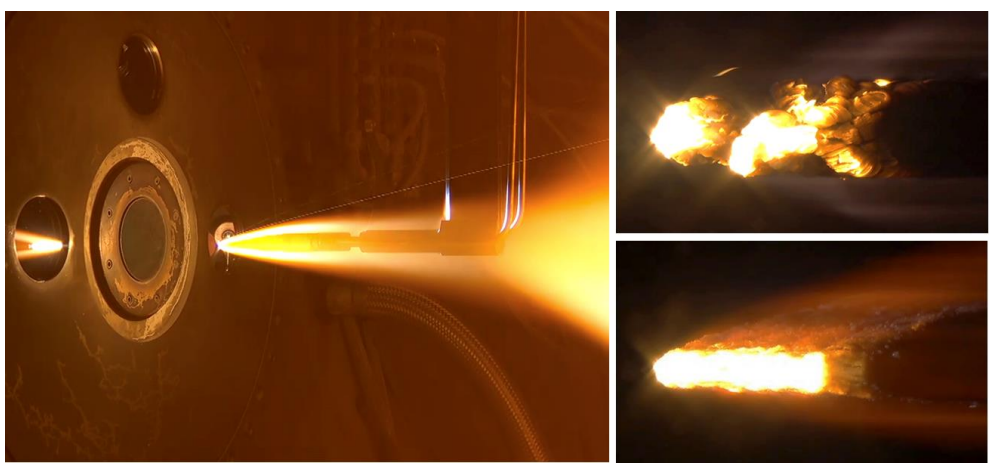

Figure 7: Test specimen during testing (left), test specimen tips of oak (top right) and TUD-WBM-2 (bottom right) at 120 s

The grey background of the temperature measurements of 1- and 2-colour pyrometer in Figure 8 illustrates the test time of 120 s. At the sample tip of TUD-WBM-2, the temperature initially rises from 1500 °C to a maximum of 2300 °C and remains relatively constant over the test duration. In contrast, the temperature measurement of the oak specimen shows clear fluctuations. This is due to a stronger degradation of the material at the test specimen tip, where the focus of the measuring spot of the temperature measurement is lost after flaking of material and is blurred or no longer on the specimen. From t = 20 s onwards, flaking of material can be detected due to strong temperature

fluctuations. After 110 s, the 2-colour pyrometer no longer measures any results and drops abruptly from 2400 °C to its starting range of 1000 °C. This is also associated with the loss of the measuring range and can be explained by the loss of the measuring spot on the material surface. The two exemplary measurement results of the temperature at the specimen tip clearly show the differences between the specimen materials due to the influence of plasma and high temperature.

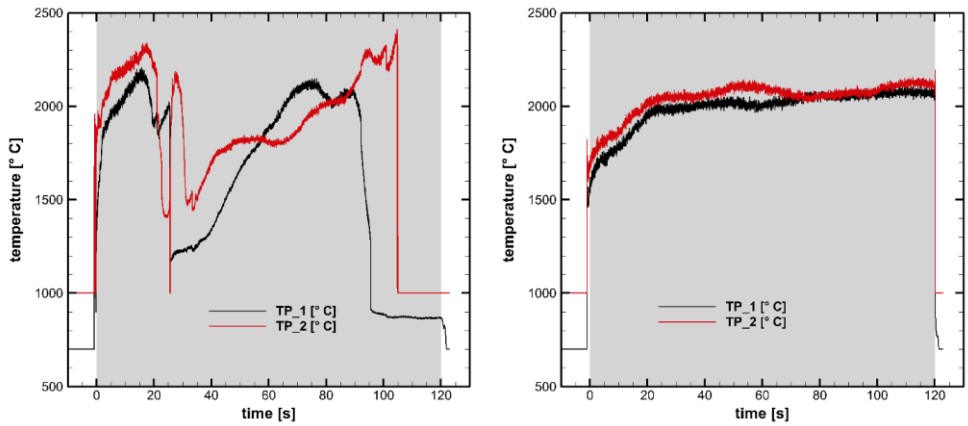

Figure 8: Temperature measurements of an oak (left) and TUD-WBM-2 (right) test specimen

Figure 9 shows a test specimen after testing on the left side. The thermographic images on the right side of Figure 9 show the strong thermal load at the test specimen tip, which decreases towards the test specimen holder. The test specimen flanks have lower temperatures than the top and bottom. The TUD-WBM-2 test specimen has a uniform, continuous tip contour after t = 60 s as well as t = 120 s, while oak has a blunt tip with discontinuous progression.

Figure 9: Test specimen after testing (left), thermographic images of oak (top right) and TUD-WBM-2 (bottom right) at 60 s

5 Post-test analysis

The analyses for evaluating the tests in L2K consist of a mass analysis, a cross-sectional area analysis and a contour analysis, which are described below.

5.1 Mass analysis

The mass of the test specimens was determined before and after the tests in L2K with a precision balance. For the mass analysis all mass fractions were related to a test time of t = 120 s. These are shown together with the results from the preliminary test (highlighted in grey) in Figure 10, sorted by ascending mass fraction after the test. The calculated densities and information on material densities from the literature or from the manufacturer are also displayed.

The wood fibre materials of the test specimens from I-WBM, TUD-WBM-1 and TUD-WBM-2 show a lower mass loss of 36 % - 47 % than the solid woods, whose mass losses range between 62 % - 73 %. Compared to the results of the preliminary test, the natural fibre-based materials have a significantly greater mass loss than the composites PTM-1 and PTM-2. TUD-WBM-2 and I-WBM surpass the solid woods tested in the preliminary test with low mass losses. All test specimens of the same material have similar results and therefore validate the material behaviour well. Their results are

summarised by their mean value in Figure 10. The TUD-WBM-2 test specimens are characterised by the lowest mass losses of all tested materials. With an average of 0.89 g/cm^3, they have a higher calculated density than the solid woods oak (0.83 g/cm^3) and mahogany (0.85 g/cm^3) from the preliminary test. They show up to 4 % less mass loss.

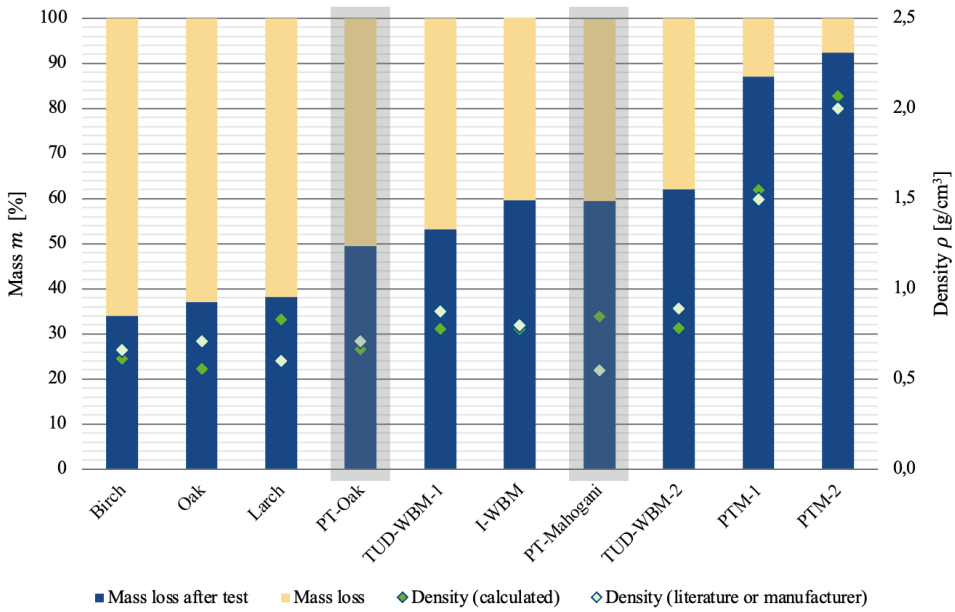

Figure 10: Results of mass analysis

5.2 Cross-sectional analysis

For the cross-sectional area analysis in the L2K test series the test specimens were cut at a distance of approximately 10 mm from the right sample flank. This distance was chosen because the samples tested in the L2K show a higher and more irregular material loss on the sample flanks. For further analysis, the large test specimen part was considered, since the cutting process damaged material parts of the gate more frequently. During the cutting process, it was found that all wood fibre materials tended to lose less charred material and had a higher structural integrity than the solid woods.

The intact cross-sectional area A_{intact}, the maximum cross-sectional area A_{max}, which results from the intact cross-sectional area and the porous char layer, as well as the original cross-sectional area $A_{original}$ are determined with the program ImageJ. Figure 11 shows examples of the superimposed

results of the cross-sectional area analysis of TUD-WBM-2 and oak compared with the original cross-sectional area $A_{original}$ before the tests in the L2K.

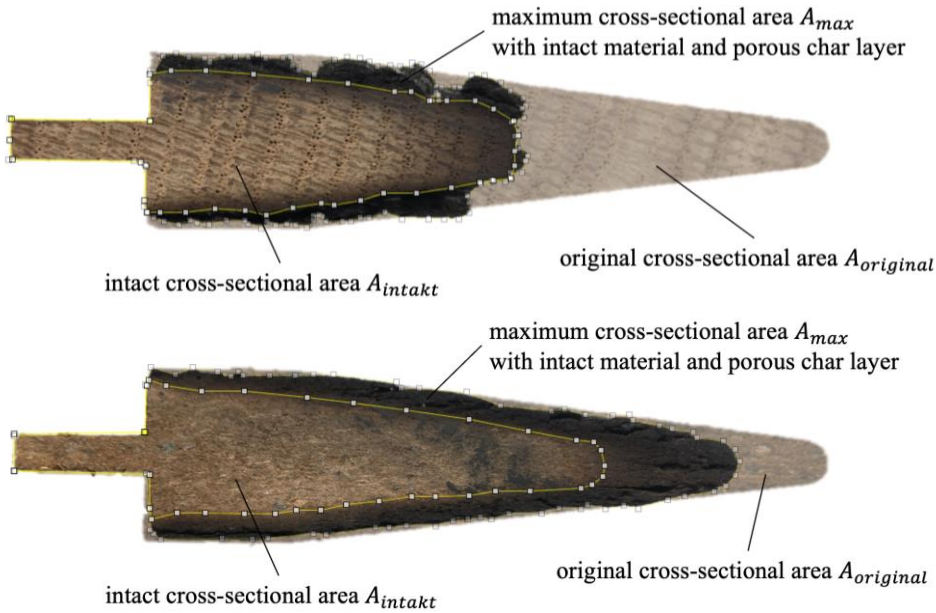

Figure 11: Cross-sectional areas of TUD-WBM-2 (top) and oak (bottom)

The percentage cross-sectional area shares related to t = 120 s are shown for all test specimens sorted by ascending maximum cross-sectional area share in Figure 12. The results of the preliminary test are highlighted in grey. Analogous to the mass analysis, the calculated densities and information on material densities from the literature or from the manufacturer are shown.

The test specimens made of wood fibre materials show a lower loss of cross-sectional area in the range of 18 % - 38 % than the solid woods, which have a loss of cross-sectional area of 48 % - 65 %. The test specimens made of wood fibre materials have the largest maximum cross-sectional areas of all tested materials after the test. The test specimens of the preliminary test are in line with the cross-sectional ratios of the solid woods. It is noticeable that the wood fibre materials have a larger maximum cross-sectional area, but the intact cross-sectional ratios overlap with the range of the solid woods (28 % - 40 %) with 30 % - 48 %. Especially samples from TUD-WBM-2 show high maximum cross-sectional areas as well as high intact cross-sectional areas, which have a porous, but still structurally intact, carbon layer.

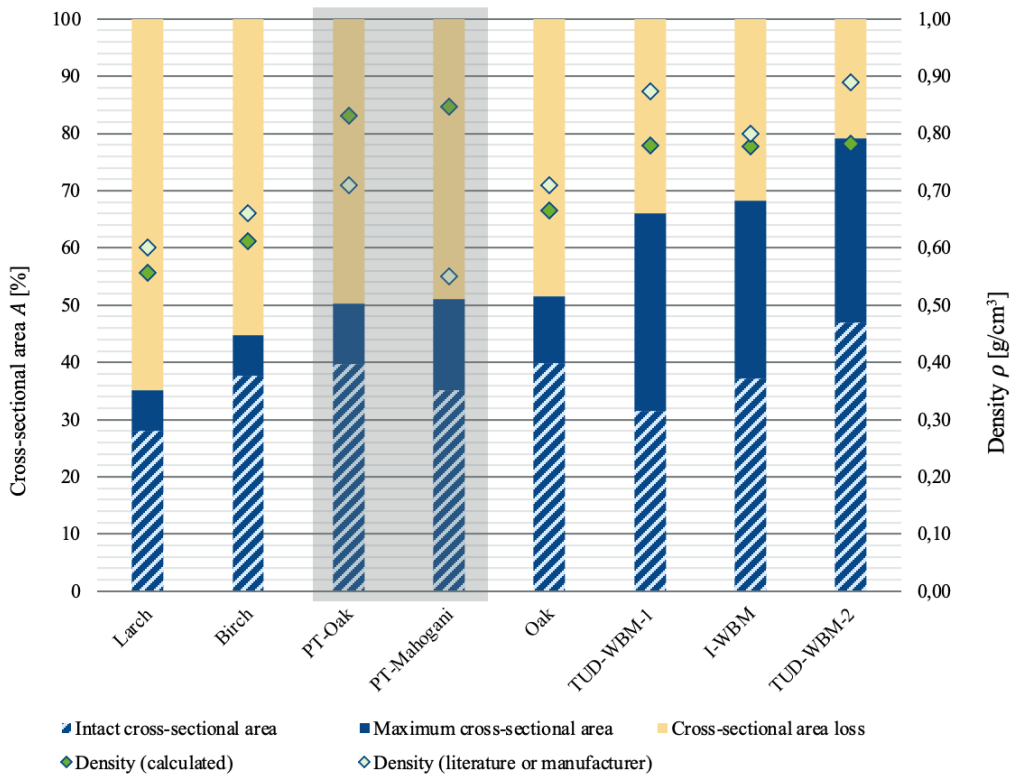

Figure 12: Results of cross-sectional area analysis

5.3 Contour analysis

For the contour analysis, the scans that recorded the contour of the test specimens before and after the test were evaluated and compared with each other. As Figure 13 shows, the test specimens were scanned in a scan holder with an angle of attack of 35°. Since the samples in the L2K are symmetrically exposed to the plasma flow, only the upper side of the samples, which represents the white part of the sample in Figure 13, can be used as an example for the contour analysis. To determine a surface contour, the samples were virtually cut along an analysis line, preferably in the centre of the specimen. In this way, a representative cut was made through the sample, which lies in the area of greatest stress on the test specimen.

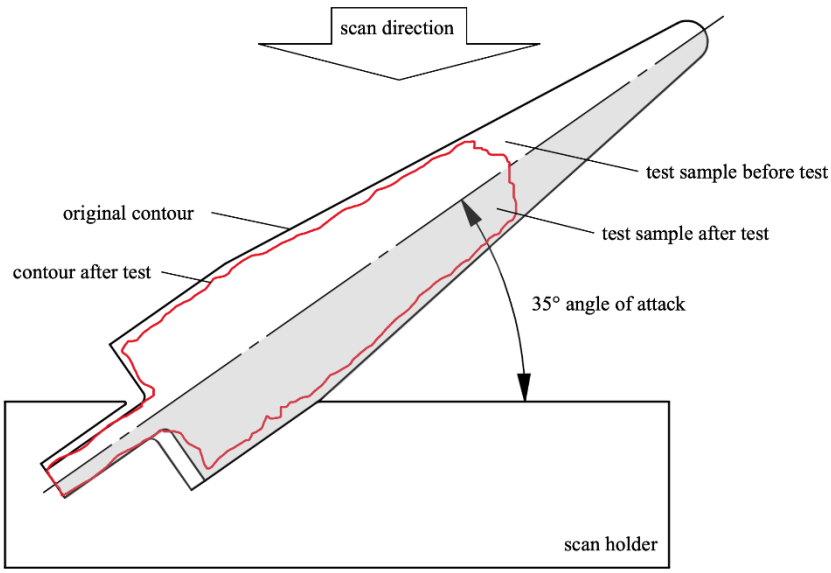

Figure 13: Scan of the surface contour of a test specimen

The contours of the upper surfaces of the test specimens Oak, TUD-WBM-1 and TUD-WBM-2 can be seen in Figure 14 and can be interpreted in the same way as in Figure 13. The original contour of the top side of the test specimen before the test is marked in black, while the surface contour after the test is marked in red. To the right of the contour curves, the top surfaces of the test specimens are shown with the analysis lines before and after the tests.

In the case of the test specimen with oak, a strong loss of material can be seen at the top of the test specimen, as the red contour line on the right-hand side drops steeply downwards. This means that the scanner no longer saw the top of the specimen but the reference surface. Compared to the black contour, the red contour runs relatively narrow. Some indentations can be seen, which can be explained by the porous carbon layer and the formation of a cracked surface. The test specimen of the solid woods show a similar contour as the test specimen from oak. A smaller loss of material can be seen in the test specimens from TUD-WBM-1 at the tip of the sample. Compared to the black contour line of the sample before the test, the sample has shrunk slightly in the thickness direction, as the red and black contours have a gap. The test specimen from TUD-WBM-2 show a loss of material at the tip of the sample, but the contour of the surface remains well preserved and dimensionally stable after the tests in the L2K, so that the red and black contours do not have

a significant distance. Small indentations due to cracks on the surface and curvatures due to melt beads are visible in the contour.

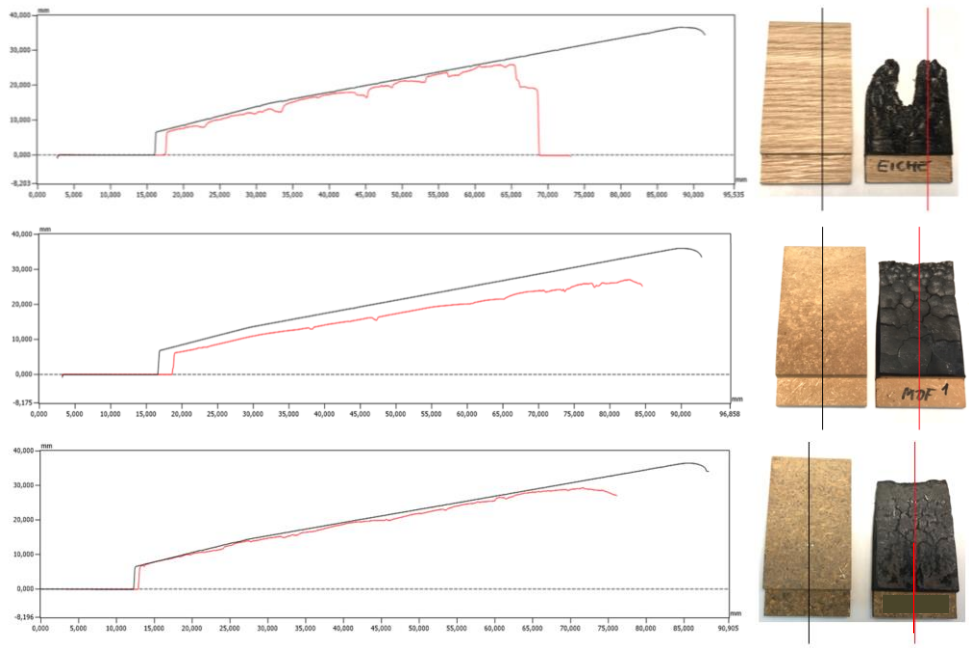

Figure 14: Results of the surface contour of the test specimens

5.4 Results and discussion

In summary, it is evident from the results of the mass and cross-sectional area analysis through the correlation of the mass after the tests and the maximum or intact cross-sectional area with the material density that the bulk density is a significant influencing factor for the resistance of the wood fibre material to thermal loads.

The tested wood fibre materials have a lower mass loss of 36 % - 47 % than solid wood (62 % - 73 %). Likewise, the cross-sectional area loss of the wood fibre materials with 18 % - 38 % is lower than that of the solid woods and cork with 48 % - 65 %. It was observed that the wood fibre samples have larger maximum cross-sectional areas after the test and therefore have a thicker porous carbon layer and pyrolysis zone. However, the intact cross-sectional ratios of the wood fibre materials (30 % - 48 %) overlap with those of the solid woods (28 % - 40 %). All tested specimens show a loss of material at the specimen tip and a shrinkage of their geometry. The specimens of TUD-

WBM-2 retain the surface contour the most in comparison with all contour courses and show the smallest changes in the specimen geometry as well as the lowest material loss. The solid woods show the biggest differences from the original contour.

Compared to the glass fibre-based CM 1 with a density of 2.0 g/cm^3 previously used by DLR, all tested fin leading edge material variants cannot yet meet the requirements for dimensional stability and geometry retention. In particular, the test specimens of TUD-WBM-2 are characterised by the lowest mass and cross-sectional area loss of all tested materials. They have the highest structural integrity of the porous carbon layer. They also have the best results of the contour analysis and, apart from the material loss at the specimen tip, show good dimensional stability and surface contour. The TUD-WBM-2 material with a density of 0.89 g/cm^3 could contribute to significant mass savings.

6 Conclusion and outlook

From the analyses and tests, it is evident that untreated wood is not an option for a use in fin leading edges of a sounding rocket. Thermal degradation is high and would jeopardise the success of the mission for a component that is part of a critical primary structure assembly.

In contrast, wood fibre materials, which are characterised by higher homogeneity, additionally containing flame-retardants, seem to be promising. Compared to solid woods, they have a higher geometry and integrity retention as well as good thermal resistance and high dimensional stability. A fanning of the leading edge could not be detected in the tests in the L2K. The wood fibre material TUD-WBM-2 seems to be particularly promising. In addition to the additive flame retardant, it could be determined by material analyses that the special natural fibre material acts as a reactive flame retardant due to a high salt content and residual components such as sand and suspended matter and delays thermal decomposition.

All wood fibre materials have low thermal conductivities and high specific thermal capacities, which reduce the transport of heat into the fin structure. Due to their production, there is a preferential direction of the fibres in the main plane of the board, which results in a significantly lower heat conductivity in the normal direction compared to in-plane conductivity. The high carbon content of the materials leads to a good ablative thermal

protection effect. Compared to the materials used so far by DLR (CM 1 and CM 2), the wood fibre materials have lower bulk densities and thus lower masses. These properties can result in a mass reduction of the rocket structure and a cost saving potential for the mission.

In summary, it can be concluded that none of the investigated material variants completely fulfils the requirements, but the wood fibre material TUD-WBM-2 can be optimised on the basis of further material analyses and thus represent the innovation potential of sustainable spaceflight materials. Detailed investigations of the mechanical material behaviour as well as the coupling of flow behaviour, dynamic structure and thermal influences can be carried out in further research. An adaptation of the geometry of the leading edge is thereby considered in order to shift the stagnation point to distribute the thermal load over a larger area.

The results of this investigation can be used to open up further areas of application with less stressed components and pave the way for transferring the findings to other sectors in which materials are exposed to high thermal stress. The potential of wood as a substitute material for establishing a bioeconomy in high-tech industries, such as the space industry, could be demonstrated.

References

[1] D. Dy, Y. Perrot, R. Pradal: *Micro-launchers: what is the market? - Quick and flexible delivery of small payloads*. PricewaterhouseCoopers PwC, 2017.

[2] G. Seibert: *The history of sounding rockets and their contribution to European space research*. in: European Space Agency, (Special Publication) ESA SP, 2006: pp. 39–46.

[3] A. Gülhan, D. Hargarten, M. Zurkaulen, F. Klingenberg, F. Siebe, S. Willems, G. Di Martino, T. Reimer: *Selected results of the hypersonic flight experiment STORT*. Acta Astronautica. 211 (2023) 333–343. https://doi.org/10.1016/j.actaastro.2023.06.034.

[4] Institut für Arbeitsschutz der Deutschen Gesetzlichen Unfallversicherung: *GESTIS-Stoffdatenbank - Natriumchlorid (NaCl).* IFA, (2022). https://gestis.dguv.de/data?name=001330.

[5] V. Tonkonogyi, V. Ivanov, J. Trojanowska, G. Oborskyi, M. Edl, I. Kuric, I. Pavlenko, P. Dašić: *Advanced Manufacturing Processes: Selected Papers from the Grabchenko's International Conference on Advanced Manufacturing Processes (InterPartner-2019)*. September 10-13, 2019, Odessa, Ukraine, 2020. https://doi.org/10.1007/978-3-030-40724-7.

[6] DIN Deutsches Institut für Normung e.V.: *DIN 68364:2003-05: Kennwerte von Holzarten (Rohdichte, Elastizitätsmodul und Festigkeiten)*. Beuth Verlag GmbH. (2003).

[7] P. Niemz: *Untersuchungen zur Wärmeleitfähigkeit ausgewählter einheimischer und fremdländischer Holzarten*. Bauphysik. 29 (2007) 311–312. https://doi.org/10.1002/bapi.200710040.

[8] DIN Deutsches Institut für Normung e.V.: *DIN EN ISO 10456: Baustoffe und Bauprodukte – Wärme- und feuchtetechnische Eigenschaften – Tabellierte Bemessungswerte und Verfahren zur Bestimmung der wärmeschutztechnischen Nenn- und Bemessungswerte*. (ISO 10456:2007 + Cor. 1:2009); Deutsche Fassung EN IS, (2010).

[9] A. Gülhan, B. Esser, U. Koch: *Experimental Investigation of Reentry Vehicle Aerothermodynamic Problems in Arc-Heated Facilities*. Journal of Spacecraft and Rockets. 38 (2001) 199–206. https://doi.org/10.2514/2.3670.

[10] A. Gülhan, B. Esser: *Arc-Heated Facilities as a Tool to Study Aerothermodynamic Problems of Reentry Vehicles*. Advanced Hypersonic Test Facilities, American Institute of Aeronautics and

Astronautics, 2002: pp. 375–403. https://doi.org/10.2514/5.9781600866678.0375.0403.

[11] A. Gülhan, B. Esser, U. Koch, K. Hannemann. *Mars entry simulation in the arc heated facility L2K*. 2002: pp. 665–672. https://elib.dlr.de/13868/.